Cement & Concrete Composites 34 (2012) 242–247

Contents lists available at SciVerse ScienceDirect

Cement & Concrete Composites

journal homepage: www.elsevier.com/locate/cemconcomp

Effect of cathodic protection on steel–concrete bond strength using ion migration measurements

J. García [a], F. Almeraya [a,e,*], C. Barrios [b], C. Gaona [c,e], R. Núñez [b], I. López [a], M. Rodríguez [c], A. Martínez-Villafañe [a], J.M. Bastidas [d]

[a] Centro de Investigación en Materiales Avanzados, S.C. (CIMAV), Departamento de Integridad y Diseño de Materiales Compuestos/Grupo Corrosión, Miguel de Cervantes 120, Complejo Ind. Chihuahua, Chihuahua, Mexico
[b] Universidad Autónoma de Sinaloa (UAS), Facultad de Ingeniería Mochis, Fuente de Poseidón y Prol. Angel Flores SN, Fracc. Las Fuentes, 81223 Los Mochis, Sinaloa, Mexico
[c] Universidad Autónoma de Chihuahua, Facultad de Ingeniería, Circuito Universitario Chihuahua, Chihuahua, Mexico
[d] Centro Nacional de Investigaciones Metalúrgicas (CENIM), CSIC, Avda. Gregorio del Amo 8, 28040 Madrid, Spain
[e] Universidad Autónoma de Nuevo León, FIME – Centro de Innovación e Investigación en Ingeniería Aeronáutica, Av. Universidad s/n, Ciudad Universitaria, San Nicolás de los Garza, Nuevo León, Mexico

ARTICLE INFO

Article history:
Received 5 April 2010
Received in revised form 21 September 2011
Accepted 21 September 2011
Available online 4 October 2011

Keywords:
Bond strength
Cathodic protection
Overprotection
Sodium
Potassium
Hydrogen ions
Concrete–steel interface

ABSTRACT

Impressed current cathodic protection (ICCP) is a widely used method to protect steel reinforcements against corrosion. Bond degradation between concrete and steel at protection and overprotection levels was studied. Two types of materials were tested: an ordinary Portland cement (OPC) and a mixture of 85% OPC and 15% fly ash (OPC/FA). Concrete specimens were immersed in a 3.5% sodium chloride (NaCl) solution. Chemical analysis of sodium, potassium and hydrogen ions was performed using atomic absorption spectrophotometry (AAS). Hydrogen ion content was monitored using electrochemical impedance spectroscopy (EIS). Mechanical behaviour was analysed by means of pullout tests, and microstructure characterisation was carried out using scanning electron microscopy (SEM). Sodium, potassium and hydrogen ions were found at the concrete–steel interface. The mechanical properties of the specimens were poorer at overprotection level than at protection level.

1. Introduction

Along with the use of corrosion inhibitors and galvanised steel or stainless steel reinforcements, cathodic protection (CP) is a reliable way of guaranteeing the durability of a reinforced concrete structure (RCS) in extremely aggressive environments. CP consists of shifting the electrode potential of a metal to a more negative value where the corrosion rate is acceptably low [1]. As a consequence the anodic reaction is suppressed:

$$Fe \rightarrow Fe^{2+} + 2e^- \quad (1)$$

and the cathodic reaction is enhanced:

$$O_2 + 2H_2O + 4e^- \rightarrow 4OH^- \quad (2)$$

$$2H^+ + 2e^- \rightarrow H_2 \quad (3)$$

thus decreasing the overall corrosion current. Oxygen reduction (Reaction (2)) is the main cathodic reaction in concrete, because concrete has a high pH and oxygen is thermodynamically a far more powerful electron acceptor than the hydrogen ion (H^+) (Reaction (3)).

The direct current (DC) for CP systems can be supplied either via mains power in an impressed current CP (ICCP) system or by a sacrificial anode in a sacrificial anode CP (SACP) system. In a SACP device, single or multiple anodes distribute the cathodic current to the protected structure.

When an electrical current is applied to the reinforcement using an external anode, the hydroxide ion (OH^-) is consumed, being oxidised to water:

$$4OH^- \rightarrow 2H_2O + O_2 + 4e^- \quad (4)$$

and producing:

$$2H_2O + O_2 + 4e^- \rightarrow 4OH^- \quad (5)$$

at the reinforcement anode. CP accuracy can be verified using the criterion of measured polarised potential values between −0.85

* Corresponding author. Address: Centro de Investigación en Materiales Avanzados, S.C. (CIMAV), Departamento de Integridad y Diseño de Materiales Compuestos/Grupo Corrosión, Miguel de Cervantes 120, Complejo Ind. Chihuahua, Chihuahua, Mexico.
E-mail address: facundo.almeraya@cimav.edu.mx (F. Almeraya).

0958-9465/$ - see front matter © 2011 Elsevier Ltd. All rights reserved.
doi:10.1016/j.cemconcomp.2011.09.014

and −1.0 V versus copper/copper sulphate electrode ($Cu/CuSO_4$) (CSE) [2].

One of the main causes of steel corrosion in RCS is chloride penetration [3]. An ICCP system to prevent or mitigate chloride-induced corrosion requires careful control because it causes a softening of calcium silicate hydrate (C–S–H) gel in the concrete matrix [4,5]. Moreover, previous studies mention that an ICCP system causes ion migration of sodium (Na^+) and potassium (K^+) towards the concrete–steel interface [6,7], which generates a bond loss between the concrete and steel, and embrittlement of the steel by hydrogen absorption.

An ICCP system can promote hydrogen activity at the concrete–steel interface and the consumption of electrons from the corrosion process, so safe CP limits need to be established in order to prevent the risk of phenomena such as hydrogen embrittlement of steel reinforcements or degradation of the concrete–steel interface. These positional variations in the cathodic current density make it difficult to maintain the same level of protection throughout the RCS. In an ICCP system with a low applied current, oxygen and potential levels may be depleted, allowing water reduction to take place:

$$2H_2O + 2e^- \rightarrow H_2 + 2OH^- \quad (6)$$

and the molecular hydrogen absorbed on the steel surface may induce the initiation of fracture damage [8].

The aim of this paper is to study the bond strength between concrete and steel as a means of assessing the ICCP on steel embedded in concrete at protection and overprotection levels. Two types of concretes were used, an ordinary Portland cement (OPC) and a blended cement obtained by replacing 15% of OPC with fly ash (OPC/FA). Sodium and potassium ion migration towards the concrete–steel interface was measured and its effect on bonding was evaluated using the pullout test. The generation of molecular hydrogen and its influence on bonding loss at the concrete–steel interface was also studied.

2. Materials and methods

A total of sixteen cylindrical test specimens were prepared, eight using type I OPC (52.5 N/SR), according to ASTM C150-09 standard [9] (OPC specimen), and eight others using 85% OPC (type I, 52.5 N/SR) and 15% fly ash, class F (from the coal-fired power plant "José López-Portillo", Rio Escondido, Coahuila, Mexico), according to ASTM C618-03 standard [10] (OPC/FA specimen). Table 1 shows the chemical composition of OPC and fly ash.

Table 2 lists the specimens used and their composition. A standard carbon steel rebar for structural concrete, with ribs and lugs, an elasticity modulus of 205 GPa, a yield strength of 370 MPa, and a nominal diameter of 0.95 cm, was placed in the axial direction with an embedded length of 10.5 cm in the centre of each cylindrical concrete specimen (of 15 cm high and 7.5 cm diameter). The exposed end of the rebar was covered with an insulating thermoplastic tape leaving an active surface area of 31.42 cm^2. The cylindrical concrete specimens were cured in water for 28 days.

After curing, the OPC and OPC/FA specimens were immersed in a 3.5% wt. NaCl solution and an ICCP system was installed. Two graphite bars with a diameter of 0.64 cm and a length of 15 cm were used as anodes. Eight of the specimens were subjected to protection level, controlling the applied current using the criterion of $-1.0\ V \leqslant E \leqslant -0.85\ V$ versus CSE, and the other eight were subjected to overprotection level using the criterion of $E < -1.0$ V versus CSE [2]. The experimental time was up to 6 months. Table 3 shows the experimental time and nomenclature of the tested concrete specimens.

Table 1
Chemical composition of the tested ordinary Portland cement (OPC) and fly ash (% mass).

Material	CaO	SiO_2	Al_2O_3	Fe_2O_3	MgO	SO_4^{2-}	Others
OPC	64.00	21.00	5.50	4.50	2.40	1.60	1.0
Fly Ash	4.59	51.78	27.80	6.18	1.52	0.71	4.51

Table 2
Studied specimens and composition using a water/cement ratio of 0.66.

Specimen	Water (kg/m^3)	Cement (kg/m^3)	Aggregate (kg/m^3)	Sand (kg/m^3)	Fly Ash (kg/m^3)
OPC	205	310	1049	781	–
OPC/FA	205	263.5	1049	781	46.5

OPC: ordinary Portland cement; OPC/FA: 85% ordinary Portland cement and 15% fly ash.

Table 3
Nomenclature of specimens tested for a period of 2–6 months.

Experimental time/months	Specimen			
2	2OPC	2OPC+	2OPC/FA	2OPC/FA+
3	3OPC	3OPC	3OPC/FA	3OPC/FA+
5	5OPC	5OPC+	5OPC/FA	5OPC/FA+
6	6OPC	6OPC+	6OPC/FA	6OPC/FA+

OPC: ordinary Portland cement at protection level; OPC+: ordinary Portland cement at overprotection level; OPC/FA: 85% ordinary Portland cement and 15% fly ash at protection level; OPC/FA+: 85% ordinary Portland cement and 15% fly ash at overprotection level.

A voltage of 6.2 V was applied in all cases. The protection level was obtained using a current of 19.2 mA and a resistance of 102.6 Ω, and the overprotection level was obtained with a current of 37.7 mA and a resistance of 71.8 Ω. Current flow was regulated using a rectifier with a capacity of 20 V/10 A to convert alternating current (AC) measurements into DC measurements.

Impedance measurements were collected at the corrosion potential (E_{corr}), imposing a 10 mV rms amplitude excitation voltage in the frequency range from 10^4 to 10^{-4} Hz and collecting 5 measurements per decade. The equipment utilised was a Frequency Response Analyser (FRA) 1260-Electrochemical Interface (EI) 1287 Solartron-Schlumberger.

The pullout test according to ASTM C900-06 standard was carried out on the cylindrical concrete specimens using a debonding plus cylinder cracking mechanism [11], with an Instron electromechanical UTM, according to ASTM E8-09 standard [12], with a load of 50 kN and operating at an across head speed from 1.7×10^{-8} to 8.3×10^{-3} m/s. Bond strength experiments were performed in triplicate.

Sodium, potassium and hydrogen ion contents were analysed. After the pullout test, one disc (10 cm diameter, 15 mm thickness) was extracted from the OPC and OPC/FA specimens and 1 g of the concrete–steel interface powder was extracted and dissolved in 100 mL of distilled water for 24 h, prior to performing chemical analysis by atomic absorption spectrophotometry (AAS) with an Avanta Sigma Spectrophotometer. The hydrogen ion content for the pullout test was also determined by implementing the antilogarithm of the pH, using the expression: $[H^+] = 10^{-pH}$.

Finally, small samples of concrete from the OPC and OPC/FA specimens were extracted from the concrete–steel interface and the surface morphology was analysed by scanning electron microscopy (SEM) using a low vacuum Jeol JSM-5800LV equipped with energy dispersive X-ray (EDX) spectrometers and with a resolution of 35 nm.

3. Results and discussion

3.1. Sodium or potassium ion content

Fig. 1a shows the potassium ion content at the concrete–steel interface versus time for the OPC and OPC/FA specimens. At the protection level the potassium ion content is very similar for both materials, of the order of 10–20 mg/L. At overprotection level the specimens show a higher potassium ion content, of the order of 30–60 mg/L, which may be attributed to the high applied current (37.7 mA). At overprotection level, the OPC + specimen shows a higher potassium ion content than the OPC/FA + specimen after 6 months of exposure, attributed to the fact that the addition of fly ash increases the amount of C–S–H gel in the cement paste. Fly ash particles react with calcium hydroxide to produce hydrated products which strongly decrease concrete porosity [13,14]. Binici et al. reported that such mechanical improvements are due to the increase in C–S–H gel volume originated by fly ash and granulated blast furnace slag (GBFS) [15].

Fig. 1b shows the sodium ion content at the concrete–steel interface versus time for the OPC and OPC/FA specimens. Here the sodium content for the OPC/FA concrete mixture at protection level is of the order of 10–45 mg/L. The sodium ion content is higher than the potassium ion content for identical experimental conditions. In a similar way to the potassium ion (Fig. 1a), sodium ion penetration is higher in the concrete specimens at overprotection level than at protection level, but here the values are high, of the order of 60–150 mg/L. This different behaviour may be attributed to the small size of the sodium ion compared to the potassium ion, and the fact that the sodium ion may present high ionic mobility in the pore network.

When the sodium or potassium ion migrates towards the concrete–steel interface, due to the applied ICCP, it displaces the calcium ion (Ca^{2+}), and reacts with the C–S–H gel (Reactions (8) and (9)) and with calcium hydroxide ($Ca(OH)_2$) (Reactions (10) and (11)) to form hydrated sodium and/or potassium silicate and sodium hydroxide (NaOH) and/or potassium hydroxide (KOH), respectively [16–22]:

$$2(3CaO \cdot SiO_2) + 6H_2O \rightarrow 3CaO \cdot 2SiO_2 \cdot 3H_2O + 3Ca(OH)_2 \quad (7)$$

$$3CaO \cdot 2SiO_2 \cdot 3H_2O + 6Na^+ \rightarrow 3Na_2O \cdot 2SiO_2 \cdot 3H_2O + 3Ca^{2+} \quad (8)$$

$$3CaO \cdot 2SiO_2 \cdot 3H_2O + 6K^+ \rightarrow 3K_2O \cdot 2SiO_2 \cdot 3H_2O + 3Ca^{2+} \quad (9)$$

$$3Ca(OH)_2 + 6Na^+ \rightarrow 6NaOH + 3Ca^{2+} \quad (10)$$

$$3Ca(OH)_2 + 6K^+ \rightarrow 6KOH + 3Ca^{2+} \quad (11)$$

Once the calcium ion has been displaced it remains in the pore solution along with the sulphate ion (SO_4^{2-}), which is a constituent of the concrete, and the chloride ion (Cl^-), which may have penetrated the concrete matrix from the outside, giving rise to a reaction between these ions to form calcium sulphate ($CaSO_4$) and/or calcium chloride ($CaCl_2$) (Reactions (12) and (13), respectively):

$$3Ca^{2+} + 3SO_4^{2-} \rightarrow 3CaSO_4 \quad (12)$$

$$3Ca^{2+} + 6Cl^- \rightarrow 3CaCl_2 \quad (13)$$

Reactions (8) and (9) produce sodium and potassium silicate gel which can absorb water and the products formed in the alkali-silica reaction [22]. This gel creates a semi-permeable membrane that has osmotic properties in the presence of water, and by means of absorption the membrane increases its volume and generates important disruptive pressures at the concrete–steel interface.

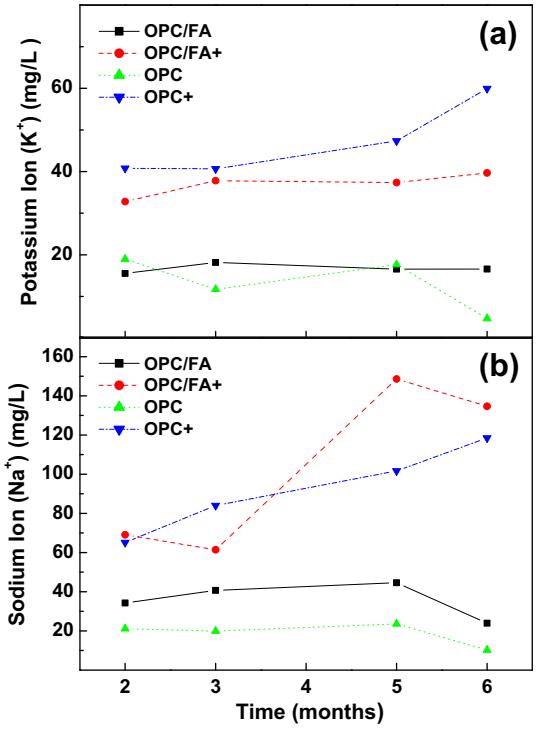

Fig. 1. Ion content at the concrete–steel interface as a function of time: (a) potassium ion and (b) sodium ion.

3.2. Pullout test measurements

Fig. 2a shows bond strength measurements versus time for OPC/FA specimens at protection (OPC/FA) and overprotection (OPC/FA+) levels. A significant decrease in bond strength can be observed at protection level 12 MPa after 2 months and 4 MPa after 6 months. The specimens at overprotection level (OPC/FA+) show variable bond strength values depending on the potassium or sodium ion content at the concrete–steel interface.

Fig. 2b shows bond strength measurements versus time for OPC specimens at protection (OPC) and overprotection (OPC+) levels. It can be seen that the OPC specimens show higher bond strength, 8.3 MPa for 2 months, than OPC + specimens, 6.3 MPa for 2 months. In general, the OPC specimens at either protection or overprotection level show little variation in bond strength over the tested experimental time. As an hypothesis, it may be suggested that the replacement of 15% OPC with FA does not improve bond properties because FA particles react slowly with $Ca(OH)_2$ and this reaction has not yet taken place.

3.3. Influence of pH on bond strength

3.3.1. Hydrogen ion content at the concrete–steel interface

Fig. 3 shows hydrogen ion content versus bond strength. Fig. 3a was obtained using the antilogarithm expression of the pH for the pullout test ($[H^+] = 10^{-pH}$). Fig. 3b was obtained using the AAS technique for powder extracted from the concrete–steel interface. Fig. 3a shows that irrespective of the type of concrete specimen, the hydrogen ion content at the concrete–steel interface decreases as the bond strength increases after 2, 3 and 5 months of exposure. In these specimens a great decrease in the hydrogen ion content is observed for bond strength values in the 8–12 MPa range. In contrast, the specimen after 6 months of exposure shows only a small decrease in the hydrogen content and low bond strength values.

Fig. 3b shows that after 2 months of exposure the specimens present a low hydrogen ion content and the highest bond strength

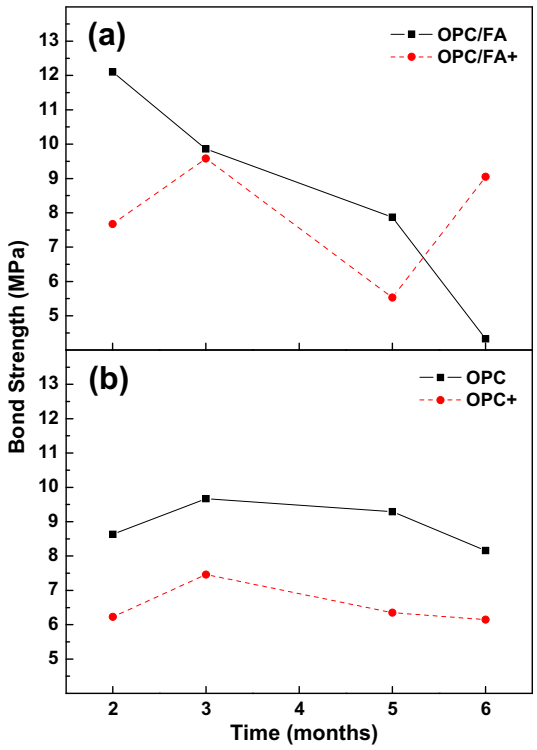

Fig. 2. Bond strength as a function of time: (a) OPC/FA specimen (85% OPC and 15% FA) at protection level (OPC/FA) and at overprotection level (OPC/FA+) and (b) OPC specimen at protection level (OPC) and at overprotection level (OPC+).

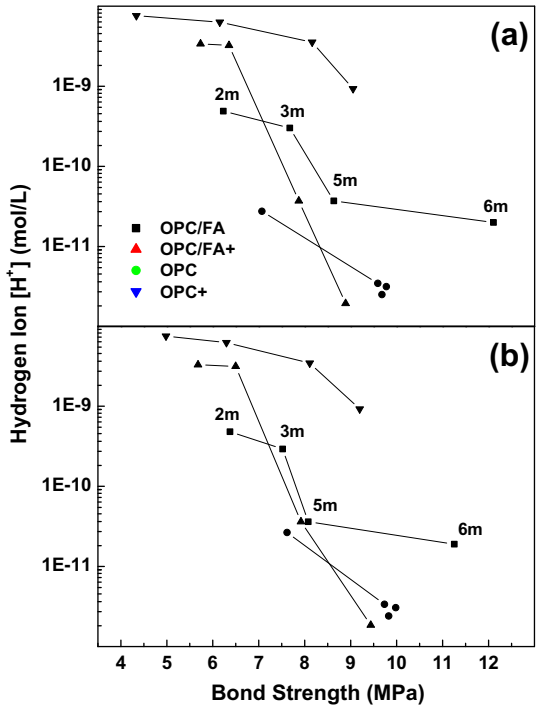

Fig. 3. Hydrogen ion content at the concrete–steel interface as a function of bond strength for 2, 3, 5 and 6 months (2 m, 3 m, 5 m and 6 m): (a) using the antilogarithm of the pH for the pullout test and (b) using the atomic absorption spectrophotometry (AAS) technique on powder extracted from the concrete–steel interface.

value. OPC/FA specimens at protection level after 2 months of exposure show a lower hydrogen ion content and a higher bond

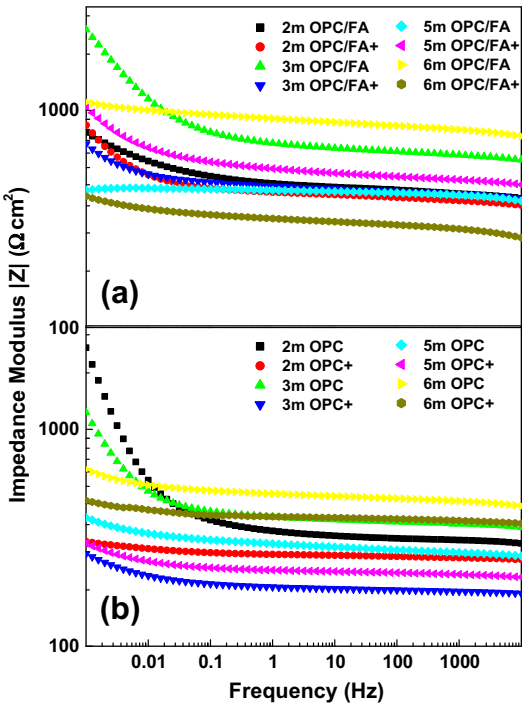

Fig. 4. Impedance modulus versus frequency diagram for 2, 3, 5 and 6 months (2 m, 3 m, 5 m and 6 m): (a) OPC/FA specimen (85% OPC and 15% FA) at protection level (OPC/FA) and at overprotection level (OPC/FA+) and (b) OPC specimen at protection level (OPC) and at overprotection level (OPC+).

strength than those at overprotection level (OPC/FA+). In general, after 5 months the specimens show similar behaviour to those after 2 months of immersion, with the exception of the OPC/FA and OPC specimens, which present contrary behaviour. It may be stated that the overprotection level generates molecular hydrogen at the concrete–steel interface [23–25]. Nevertheless, the OPC/FA specimens at protection level after 6 months show a low bond strength and a higher hydrogen content than after 2, 3 and 5 months. It may be indicated that the accumulation of hydrogen decreases as the pH of the concrete drops, therefore losing bond properties at the concrete–steel interface. The high bond of the OPC/FA specimens could be due to a confinement process [26]. The application of an overprotection level may enhance molecular hydrogen evolution at the concrete–steel interface.

3.3.2. Hydrogen ion content using impedance data

Fig. 4a shows the impedance modulus versus frequency diagram for OPC/FA specimens at protection (OPC/FA) and overprotection (OPC/FA+) levels. Fig. 4b shows similar information referring to OPC specimens. As can be observed, the impedance modulus varies little from one specimen to another, and the OPC/FA specimens present a higher impedance modulus than the OPC specimens. The OPC/FA specimens have a lower hydrogen content due to the reaction between fly ash particles and calcium hydroxide to generate hydrated products in the cement paste. This process improves their mechanical properties.

Fig. 4b shows that the OPC specimens at protection level (OPC) present a higher impedance modulus than those at overprotection (OPC+) level. Thus, there is less hydrogen ion migration towards the concrete–steel interface on the specimens at protection level. High hydrogen migration lowers the pH of the concrete and thus depletes mechanical properties at the concrete–steel interface. This difference in behaviour may be attributed to the easy migration of hydrogen towards the concrete–steel interface [8].

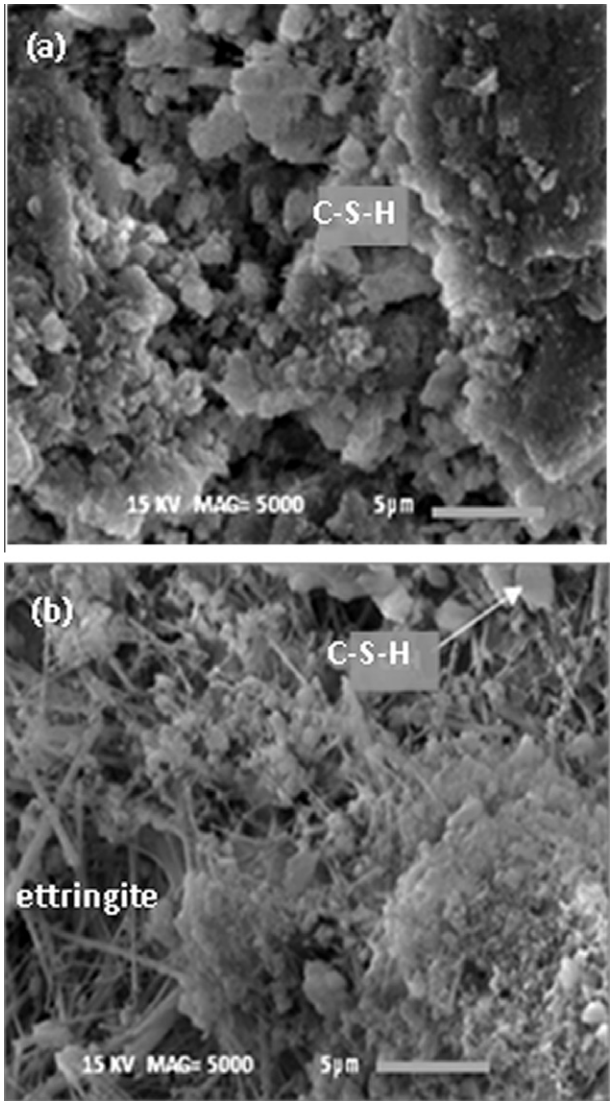

Fig. 5. Scanning electron microscopy (SEM) image: (a) OPC/FA specimen (85% OPC and 15% FA); (b) OPC specimen including C–S–H gel and ettringite.

3.4. Scanning electron microscopy

Fig. 5a shows a SEM image for an OPC/FA specimen at protection level after 6 months of exposure. Fig. 5b shows a SEM image for an OPC specimen at protection level after 6 months of exposure. It can be observed that the amount of C-S-H gel formed by cement hydration in an OPC specimen at protection level is smaller than in an OPC/FA specimen. Therefore, the reduction in the amount of C–S–H gel in the OPC specimens may be responsible for their poor bond strength (see Fig 5b). The OPC specimens also contain needle-shaped ettringite ($Ca_6Al_2(SO_4)_3(OH)_{12} \cdot 26H_2O$) as a hydration product with a harmful influence. The addition of FA particles may lead to an increase in the amount of C–S–H gel [15,27], and therefore increase the bond strength at the concrete–steel interface. There is a visible difference between the specimens manufactured with OPC/FA and OPC, since the OPC/FA specimens present a more homogeneous, compact and dense microstructure than the OPC specimens, meaning an increase in the bond strength.

4. Conclusions

Potassium, sodium and hydrogen ion migration towards the concrete–steel interface plays an important role in bond loss between steel and concrete in structures under cathodic protection by the impressed current method. The potassium ion content is lower in concrete specimens at protection level containing fly ash, due to its reaction with calcium hydroxide, while sodium ion migration is higher in concrete containing fly ash, which is attributed to the small size of the sodium ion. At overprotection level the potassium and sodium ions migrate more easily than at protection level. At overprotection level the hydrogen content is higher than at protection level, which is attributed to the generation of molecular hydrogen at overprotection level. The impedance modulus versus frequency diagram shows the effect of the overprotection level, relating Ohm's law with the hydrogen ion content. The overprotection level yields the lowest impedance modulus and bond strength. The SEM image shows that the presence of C–S–H gel is higher in the specimens with fly ash than in those without fly ash.

Tests conducted at different ages indicated that the OPC specimens at either protection or overprotection level show little variation in bond strength with time. The OPC/FA specimens at protection level show 12 MPa for 2 months and 4 MPa for 6 months. At overprotection level (OPC/FA+) the bond strength depends on the potassium or sodium ion content. Hydrogen ion content for OPC/FA specimens decreases as the bond strength increases after 2, 3 and 5 months. In contrast, the specimen after 6 months of exposure shows only a small decrease in the hydrogen content and low bond strength values.

Acknowledgements

J. Garcia expresses his gratitude to the CONACYT of Mexico for the scholarship granted to him. Thanks to A. Borunda-Terrazas, V. Orozco-Campos, W. Antunez and E. Torres-Molle for their technical assistance. JM Bastidas expresses his gratitude to Project BIA2008-05398 from the CICYT, Spain, for financial support.

References

[1] Montoya R, Aperador W, Bastidas DM. Influence of conductivity on cathodic protection of reinforced alkali-activated slag mortar using the finite element method. Corros Sci 2009;51(12):2857–62.
[2] Funahashi M, Bushman JB. Technical review of 100 mV polarization shift criterion for reinforcing steel in concrete. Corrosion 1991;47(5):376–86.
[3] Andrade C. Calculation of chloride diffusion coefficients in concrete from ionic migration measurements. Cem Concr Res 1993;23(3):724–42.
[4] Dehghanian C. Effect of impressed current on bond strength between steel rebar and concrete. Int J Eng 1998;11(3):121–34.
[5] Chang JJ, Yeih W, Huang R. Degradation of the bond strength between rebar and concrete due to the impressed cathodic current. J Mater Sci Tech 1999;7(2):89–93.
[6] Chang JJ. A study of the bond degradation of rebar due to cathodic protection current. Cem Concr Res 2002;32(4):657–63.
[7] Rasheeduzzafar MGA, Alsulaimani GJ. Degradation of bond between reinforcing steel and concrete due to cathodic protection current. ACI Mater J 1993;90(1):8–15.
[8] Zampronio MA, Fassini FD, Miranda PEV. Design of ion-implanted hydrogen contamination barrier layers for steel. Surf Coat Technol 1995;70(2–3):203–9.
[9] ASTM C150-09 Standard. Standard specification for Portland cement. doi: 10.1520/C0150-C0150M-09.
[10] ASTM C618-03 Standard. Standard specification for coal fly ash and raw or calcined natural pozzolan for use in concrete. doi: 10.1520/C0618-08A.
[11] ASTM C900-06 Standard. Standard test method for pullout strength of hardened concrete. doi: 10.1520/C0900-06.
[12] ASTM E8-09 Standard. Standard test methods for tension testing of metallic materials. doi: 10.1520/E0008-E0008M-09.
[13] Garcés P, Andión LG, Zornoza E, Bonilla M, Payá J. The effect of processed fly ashes on the durability and the corrosion of steel rebars embedded in cement-modified fly ash mortars. Cem Concr Compos 2010;32(3):204–10.
[14] Fraay ALA, Bijen JM, de Haan YM. The reaction of fly ash in concrete a critical examination. Cem Concr Res 1989;19(2):235–46.
[15] Binici H, Cagatay IH, Shah T, Kapur S. Mineralogy of plain Portland and blended cement pastes. Build Environ 2008;43(7):1318–25.
[16] Ponce JM, Batic OR. Different manifestations of the alkali-silica reaction in concrete according to the reaction kinetics of the reactive aggregate. Cem Concr Res 2006;36(6):1148–56.

[17] Ben-Haha M, Gallucci E, Guidoum A, Scrivener KL. Relation of expansion due to alkali silica reaction to the degree of reaction measured by SEM image analysis. Cem Concr Res 2007;37(8):1206–14.
[18] García-Díaz E, Riche J, Bulteel D, Vernet C. Mechanism of damage for the alkali-silica reaction. Cem Concr Res 2006;36(2):395–400.
[19] Leemann A, Lothenbach B. The influence of potassium–sodium ratio in cement on concrete expansion due to alkali-aggregate reaction. Cem Concr Res 2008;38(10):1162–8.
[20] Hobbs DW. Influence of mix proportions and cement alkali content upon expansion due to the alkali-silica reaction. Technical Report 534. Wexham Springs, UK: Cement and Concrete Association; 1980.
[21] Swamy NR, Al-Asali MM. Expansion of concrete due to alkali silica reaction. ACI Mater J 1988;85(1):33–40.
[22] MacGowan JK, Vivian HE. Studies in cement-aggregate reaction. Correlation between crack and expansion of mortars. Aust J Appl Sci 1952;3(4):228–32.
[23] Pangrazzi R, Hartt WH, Kessler R. Cathodic polarization and protection of simulated prestressed pilings in seawater. Corrosion 1994;50(3):186–96.
[24] Scannell W, Sohanghpurwala A, Powers R, Hartt W. Cathodic protection of prestressed concrete bridge piles in a marine environment. Corrosion/94. paper No. 305, Houston, TX; 1994.
[25] Hu RP, Manolatos P, Jerome M, Meyer M, Galland J. Hydrogen absorption by cathodically protected underground steel piping in thiosulfate containing media. Corros Sci 1998;40(4–5):619–29.
[26] Yeih W, Huang R, Chang JJ, Yang CC. A Pullout test for determining interface properties between rebar and concrete. Adv Cem Based Mater 1997;5(2):57–65.
[27] Yoon-Seok C, Jung-Gu K, Kwang-Myong L. Corrosion behavior of steel bar embedded in fly ash concrete. Corros Sci 2006;48(7):1733–45.